

Amine-Catalyzed B–O–C Bond Formation: Mechanistic Insights from Density Functional Theory and Second-Order Møller–Plesset Perturbation Theory

Krishna L. Bhat,[§] Jack H. Lai,[#] George D. Markham,[†] Anthony M. DiJulio,^{†,‡} and Charles W. Bock^{*,§,†}

Department of Chemistry and Biochemistry, School of Science and Health, Philadelphia University, School House Lane and Henry Avenue, Philadelphia, Pennsylvania 19144, Department of Biochemistry, Tufts University School of Medicine, 136 Harrison Avenue, Boston, Massachusetts 02111, The Institute for Cancer Research, Fox Chase Cancer Center, 333 Cottman Avenue, Philadelphia, Pennsylvania 19111, and Department of Chemistry, Muhlenberg College, 2400 Chew Street, Allentown, Pennsylvania 18104

Received October 24, 2005

Boronic acids react with compounds containing 1,2- or 1,3-diols to form five- or six-membered cyclic boronate esters, respectively, although many factors that influence these reactions are not well understood. In the present study, density functional theory and second-order Møller–Plesset (MP2) perturbation theory were employed to examine the mechanism in which a primary aliphatic amine acts as an internal Lewis base to catalyze the formation of a boron–oxygen–carbon linkage in the methanolysis of $\text{H}_2\text{N}-\text{CH}_2-\text{CH}=\text{CH}-\text{B}(\text{OH})_2$ to afford $\text{H}_2\text{N}-\text{CH}_2-\text{CH}=\text{CH}-\text{B}(\text{OH})(\text{OCH}_3)$; solvent effects were assessed using the polarized continuum model and explicit water molecules. In vacuo, the lowest-energy conformer of $\text{H}_2\text{N}-\text{CH}_2-\text{CH}=\text{CH}-\text{B}(\text{OH})_2$ was a seven-membered, hydrogen-bonded ring structure in which the boronic acid moiety had a planar, trigonal geometry. The catalytic role of the primary amine group in the methanolysis of $\text{H}_2\text{N}-\text{CH}_2-\text{CH}=\text{CH}-\text{B}(\text{OH})_2$ results from facilitation of a proton transfer from an intermolecular B–O dative-bonded adduct between methanol and this boronic acid, rather than from the formation of an intramolecular B–N dative bond. In the absence of amine catalysis, transition states for the rate-determining proton-transfer step in this methanolysis are 12.8–17.3 kcal/mol higher in energy. In the reaction field of water, a five-membered B–N dative-bonded ring conformer of $\text{H}_2\text{N}-\text{CH}_2-\text{CH}=\text{CH}-\text{B}(\text{OH})_2$ was lowest in energy at the MP2 level, but hydrated zwitterionic structures also appear to play an important role in this complex aminoboronic acid/methanol association and ether formation. In contrast to the PBE1PBE functional, B3LYP gave anomalous results for some steps in the methanolysis when compared with those from the more robust, albeit expensive, ab initio MP2 method.

Introduction

Organoboronic acids are becoming increasingly important as pharmaceutical agents, where they have been used for the development of selective transporters of nucleosides, saccharides, and nucleotides,^{1–4} as inhibitors of proteases,^{5–11} and as

therapeutic agents in boron neutron capture therapy (BNCT) for certain types of brain tumor.^{12,13} Recently, some boronic acids have shown significant anti-HIV activity,¹⁴ although the mechanistic details of this activity have not yet been reported. In synthetic medicinal chemistry, boronic acids are important intermediates that have been widely used in Suzuki cross-coupling¹⁵ and Diels–Alder¹⁶ reactions; they are also employed for the protection of diols,^{17,18} for selective reduction of aldehydes,¹⁹ for carboxylic acid activation,^{20,21} for the asymmetric syntheses of amino acids,²² and as templates in a variety of synthetic protocols.²³ One of the more novel uses of boronic

* Corresponding author. Tel: (215) 951-2876. Fax: (215) 951-6812. E-mail: bockc@philau.edu.

[§] Philadelphia University.

[#] Tufts University School of Medicine.

[†] Fox Chase Cancer Center.

[‡] Muhlenberg College.

(1) Mohler, L. K.; Czarnik, A. W. *J. Am. Chem. Soc.* **1993**, *115*, 2998.
(2) Paugam, M.-F.; Bien, J. T.; Smith, B. D.; Chrisstoffels, L. A. J.; de Jong, F.; Reinhoudt, D. N. *J. Am. Chem. Soc.* **1996**, *118*, 9820.

(3) Riggs, J. A.; Hossler, K. A.; Smith, B. D.; Karpa, M. J.; Griffin, G.; Duggan, P. *J. Tetrahedron Lett.* **1996**, *37*, 6303.

(4) Westmark, P. R.; Gardiner, S. J.; Smith, B. D. *J. Am. Chem. Soc.* **1996**, *118*, 11093.

(5) Adams, J.; Behnke, M.; Chen, S.; Cruickshank, A. A.; Dick, L. R.; Grenier, L.; Klunder, J. M.; Ma, Y. T.; Plamondon, L.; Stein, R. L. *Bioorg. Med. Chem. Lett.* **1998**, *8*, 333.

(6) Bao, D. H.; Huskey, W. P.; Kettner, C. A.; Jordan, F. *J. Am. Chem. Soc.* **1999**, *121*, 4684.

(7) Myung, J.; Kim, K. B.; Crews, C. M. *Med. Res. Rev.* **2001**, *21*, 245.

(8) Suenaga, H.; Yamamoto, H.; Shinkai, S. *Pure Appl. Chem.* **1996**, *68*, 2179.

(9) Teicher, B. A.; Ara, G.; Herbst, R.; Palombella, V. J.; Adams, J. *Clin. Cancer Res.* **1945**, *5*, 2638.

(10) Tian, Z. Q.; Brown, B. B.; Mack, D. P.; Hutton, C. A.; Bartlett, P. A. *J. Org. Chem.* **1997**, *62*, 514.

(11) Weston, G. S.; Blazquez, J.; Baquero, F.; Shoichet, B. K. *J. Med. Chem.* **1998**, *41*, 4577.

(12) Spievogel, R.; Gopalaswamy, S.; Sanka, P. D.; Boyle, G.; Head, K.; Devito, K. *J. Chem. Soc., Perkin Trans. 2* **2000**, *2*, 557.

(13) Srivastava, R. R.; Singhaus, R. R.; Kabalka, G. W. *J. Org. Chem.* **1999**, *64*, 8495.

(14) Yang, W.; Gao, X.; Wang, B. *Med. Res. Rev.* **2003**, *23*, 346.

(15) Miyaura, N.; Suzuki, A. *Chem. Rev.* **1995**, *95*, 2457.

(16) Ishihara, K.; Yamamoto, H. *Eur. J. Org. Chem.* **1999**, *527*, 7.

(17) Ferrer, R. J. *Adv. Carbohydr. Chem. Biochem.* **1978**, *35*, 31.

(18) Oshima, K.; Aoyama, Y. *J. Am. Chem. Soc.* **1999**, *121*, 2315.

(19) Yu, H.; Wang, B. *Synth. Commun.* **2001**, *31*, 2719.

(20) Latta, R.; Springsteen, G.; Wang, B. H. *Synthesis (Stuttgart)* **2001**, 1611.

(21) Yang, W.; Gao, G.; Springsteen, G.; Wang, B. *Tetrahedron Lett.* **2002**, *43*, 6339.

(22) Petasis, N. A.; Zavialov, I. A. *J. Am. Chem. Soc.* **1997**, *119*, 445.

acid derivatives is in the development of fluorescent and colorimetric sensors for polyols,^{24–28} where the boronic acid moiety is utilized as a recognition motif because of its strong interactions with diols.²⁶ In addition, the formation of cyclic boronate esters from chiral diols yields a remarkably high resolution of diastereotopic proton NMR signals, a property useful for the determination of the enantiomeric integrity of the chiral diols.²⁹

The boronic acid–diol complexation process has been studied experimentally for many years.^{26,30–40} These studies have shown that formation of the resulting five- or six-membered cyclic boronate ester is fast when the boron atom is initially in a tetrahedral (sp^3) environment, which occurs in basic aqueous media.⁴¹ Wulff⁴² was the first to demonstrate that an amino group in the vicinity of the boronic acid functionality can act as an *internal* Lewis base and lower the working pH of a boronic acid-based sensor molecule. Subsequently, other neighboring groups such as acetamido, pyridine, thiourea, and acetamidine have been shown to be effective in a similar capacity.⁴³ This finding has been exploited in recent years to develop practical molecular fluorescence saccharide sensors that function at, or near, neutral pH.^{26,39,44}

Many mechanistic factors associated with the formation of boron–oxygen–carbon (B–O–C) bonds formed during the reaction of a boronic acid and a vicinal diol are not well understood, particularly when an internal nitrogenous Lewis base is in the proximity of the boronic acid group.^{40,45} In this article, we present results from a computational study using both density functional theory and second-order Møller–Plesset perturbation theory to elucidate the mechanism involved in the formation of a B–O–C linkage during the reaction of an aminoboronic acid and a simple aliphatic alcohol; using a monol in place of a 1,2- or 1,3-diol simplifies the calculations and focuses attention on the formation of this linkage by eliminating issues such as the differentiation between “stepwise” and “concerted” mechanisms

for the formation of the cyclic boronic esters.⁴⁶ In particular, we investigate the reaction of (3-amino-1-propenyl)dihydroxy borane, $H_2N-CH_2-CH=CH-B(OH)_2$, and methanol, H_3C-OH , that forms [(3-amino-1-propenyl)monohydroxy]borane methyl ether, $H_2N-CH_2-CH=CH-B(OH)(OCH_3)$, and water; the primary amine group in the reactant acid has the potential to act as an internal Lewis base⁴¹ and catalyze the methanolysis. In this study we provide a detailed analysis of the structure of the aminoboronic acid $H_2N-CH_2-CH=CH-B(OH)_2$ and discuss its interaction with methanol.

Computational Methods

Geometry optimizations of the molecules in this study were performed using density functional theory (DFT) and second-order Møller–Plesset perturbation theory (MP2) in which all the electrons were included in the correlation calculation.⁴⁷ Two different hybrid functionals were employed in this study: (1) B3LYP, Becke’s three-parameter hybrid method that uses the dynamical correlation functional of Lee, Yang, and Parr,^{48,49} and (2) PBE1PBE, a one-parameter generalized gradient approximation (GGA) that uses the PBE functional with a 25% exchange and 75% correlation weighting.^{50,51} The GAUSSIAN 03 suite of programs⁵² was employed throughout, and the internally stored 6-311++G** basis set, which includes polarization and diffuse functions on all atoms, was used for the final optimizations.^{53–55} Frequency analyses were carried out to determine whether the optimized structures were local minima or transition states on the potential energy surface (PES) and to evaluate thermal contributions necessary for the calculation of reaction enthalpies and free energies at 298 K. Intrinsic reaction coordinate calculations were performed for the transition states in this study to clearly identify the corresponding local minima. Atomic charges were obtained from natural population analyses (NPA), and the wave functions were analyzed with the aid of natural bond orbitals (NBOs).^{56–60}

- (23) Currie, G. S.; Drew, M. G. B.; Harwood, L. M.; Hughes, D. J.; Luke, R. W. A.; Vickers, R. J. *J. Chem. Soc., Perkin Trans.* **2000**, 1, 2982.
 (24) James, T. D.; Sandanayake, K. R. A. S.; Shinkai, S. *Angew. Chem., Int. Ed. Engl.* **1996**, 35, 1910.
 (25) Ni, W.; Fang, G.; Springsteen, B.; Wang, B. *J. Org. Chem.* **2004**, 69, 1999.
 (26) Wang, W.; Gao, X.; Wang, B. *Curr. Org. Chem.* **2002**, 6, 1285, and references therein.
 (27) Yang, W.; Gao, S.; Gao, X.; Karnati, V. V.; Ni, W.; Wang, B.; Hooks, W. B.; Carson, J.; Weston, B. *Bioorg. Med. Chem. Lett.* **2002**, 12, 2175.
 (28) Yoon, J.; Czarnik, J. J. *Am. Chem. Soc.* **1992**, 114, 5874.
 (29) Caselli, E.; Danieli, C.; Morandi, S.; Bonfiglio, B.; Forni, A.; Prati, F. *Org. Lett.* **2003**, 5, 4863.
 (30) Brown, H. C.; Vara Prasad, J. V. N. *J. Org. Chem.* **1986**, 51, 4526.
 (31) Lauer, M.; Wulff, G. *J. Organomet. Chem.* **1983**, 256, 1.
 (32) Pizer, R.; Ricatto, P. J. *Inorg. Chem.* **1994**, 33, 2402.
 (33) Pizer, R. D.; Ricatto, P. J.; Tihal, C. A. *Polyhedron* **1993**, 12, 2137.
 (34) Springsteen, G.; Wang, B. *Chem. Commun.* **2001**, 1608.
 (35) Springsteen, G.; Wang, B. H. *Tetrahedron* **2002**, 58, 5291.
 (36) Van Duin, M.; Peters, J. A.; Kieboom, A. P. G.; Van Bekkum, H. *Tetrahedron* **1984**, 40, 2901.
 (37) Van Duin, M.; Peters, J. A.; Kieboom, A. P. G.; Van Bekkum, H. *Tetrahedron* **1985**, 41, 3411.
 (38) Wang, W.; Yan, J.; Fang, H.; Wang, B. *Chem. Commun.* **2003**, 792.
 (39) Wang, W.; Yan, J.; Springsteen, G.; Deeter, S.; Wang, B. *Bioorg. Med. Chem. Lett.* **2003**, 13, 1019.
 (40) Arimori, S.; James, T. D. *Tetrahedron Lett.* **2002**, 43, 507.
 (41) Wiskur, S. L.; Lavigne, J. J.; Ait-Haddou, H.; Lynch, V.; Chiu, Y. H.; Canary, J. W.; Anslyn, E. V. *Org. Lett.* **2001**, 3, 1311.
 (42) Wulff, G. *Appl. Chem.* **1982**, 54, 2093.
 (43) Bierdrzycki, M.; Scouten, W. H.; Bierdrzycka, Z. *J. Organomet. Chem.* **1992**, 431, 255.
 (44) James, T. D.; Shinkai, S. *Top. Curr. Chem.* **2002**, 218, 159.
 (45) Wang, W.; Springsteen, G.; Gao, S. H.; Wang, B. H. *J. Chem. Soc., Chem. Commun.* **2000**, 1283.

- (46) Bhat, K. L.; Hakik, S.; Carvo, J. N.; Marycz, D. M.; Bock, C. W. *J. Mol. Struct. (THEOCHEM)* **2004**, 673, 145.
 (47) Møller, C.; Plesset, M. S. *Pure Appl. Chem.* **1934**, 46, 618.
 (48) Becke, A. D. *J. Chem. Phys.* **1993**, 98, 5648.
 (49) Lee, C.; Yang, W.; Parr, R. G. *Phys. Rev. B: Condens. Matter* **1988**, 37, 785.
 (50) Bhat, K. L.; Braz, V.; Laverty, E.; Bock, C. W. *J. Mol. Struct. (THEOCHEM)* **2004**, 712, 9.
 (51) Perdew, J. P.; Burke, K.; Ernzerhof, M. *Phys. Rev. Lett.* **1997**, 78, 1396.
 (52) Frisch, M. J.; Trucks, G. W.; Schlegel, H. B.; Scuseria, G. E.; Robb, M. A.; Cheeseman, J. R.; Montgomery, J. A., Jr.; Vreven, T.; Kudin, K. N.; Burant, J. C.; Millam, J. M.; Iyengar, S. S.; Tomasi, J.; Barone, V.; Mennucci, B.; Cossi, M.; Scalmani, G.; Rega, N.; Petersson, G. A.; Nakatsuji, H.; Hada, M.; Ehara, M.; Toyota, K.; Fukuda, R.; Hasegawa, J.; Ishida, M.; Naskajima, T.; Honda, Y.; Kitao, O.; Nakai, H.; Klene, M.; Li, X.; Knox, J. E.; Hratchian, H. P.; Cross, J. B.; Adamo, C.; Jaramillo, J.; Gomperts, R.; Stratmann, R. E.; Yazyev, O.; Austin, A. J.; Cammi, R.; Pomelli, C.; Ochterski, J. W.; Ayala, P. Y.; Morokuma, K.; Voth, G. A.; Salvador, P.; Dannenberg, J. J.; Zakrzewski, V. G.; Dapprich, S.; Daniels, A. D.; Strain, M. C.; Farkas, O.; Malick, D. K.; Rabuck, A. D.; Raghavachari, K.; Foresman, J. B.; Ortiz, J. V.; Cui, Q.; Baboul, A. G.; Clifford, S.; Cioslowski, J.; Stefanov, B. B.; Liu, G.; Liashenko, A.; Piskorz, P.; Komaromi, I.; Martin, R. L.; Fox, D. J.; Keith, T.; Al-Laham, M. A.; Peng, C. Y.; Nanayakkara, A.; Challacombe, M.; Gill, P. M. G.; Johnson, B.; Chen, W.; Wong, M. W.; Gonzalez, C.; Pople, J. A.; *Gaussian 03*, Rev. B.02; Gaussian Inc.: Pittsburgh, PA, 2003.
 (53) Gordon, M. S. *Chem. Phys. Lett.* **1980**, 76, 163.
 (54) Hariharan, P. C.; Pople, J. A. *Theor. Chim. Acta* **1973**, 28, 213.
 (55) Hehre, W. J.; Ditchfield, R.; Pople, J. A. *J. Chem. Phys.* **1972**, 56, 2257.
 (56) Carpenter, J. E.; Weinhold, F. *J. Mol. Struct. (THEOCHEM)* **1988**, 169, 41.
 (57) Foster, J. P.; Weinhold, F. *J. Am. Chem. Soc.* **1980**, 102, 7211.
 (58) Reed, A. E.; Curtiss, L. A.; Weinhold, F. *Chem. Rev.* **1988**, 88, 899.
 (59) Reed, A. E.; Weinhold, F. *J. Chem. Phys.* **1983**, 78, 4066.
 (60) Reed, A. E.; Weinstock, R. B.; Weinhold, F. *J. Chem. Phys.* **1985**, 83, 735.

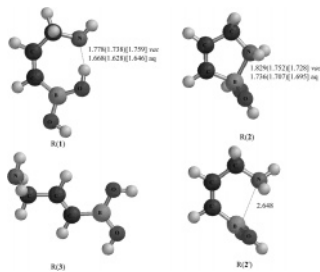


Figure 1. Optimized structures of conformers R(1)–R(3) of $\text{H}_2\text{N}-\text{CH}_2-\text{CH}=\text{CH}-\text{B}(\text{OH})_2$. (Atomic distances are given in angstroms (Å) at the B3LYP(PBE1PBE)[MP2] computational levels.)

To examine the influence of an aqueous environment on the methanolysis of $\text{H}_2\text{N}-\text{CH}_2-\text{CH}=\text{CH}-\text{B}(\text{OH})_2$, self-consistent reaction field (SCRf) optimizations were performed on various conformers of the reactants, products, and intermediates involved in the process. These SCRf calculations were carried out using the IEF polarizable continuum model (PCM) with radii obtained from the universal force field (UFF), as implemented in GAUSSIAN 03.^{52,61–64} Since continuum methods have some well-established limitations in describing protic solvents,^{65,66} SCRf calculations that include an *explicit* water molecule were performed in a few cases.

Results and Discussion

Total molecular energies, thermal corrections to 298 K, and entropies for the molecules in this article are listed in Table 1S of the Supporting Information.

A. Structure of $\text{H}_2\text{N}-\text{CH}_2-\text{CH}=\text{CH}-\text{B}(\text{OH})_2$. Despite the burgeoning interest in boronic acid chemistry, there are relatively few experimental or computational data on the structure of aminoboronic acids in which there is the potential to form an intramolecular B–N dative bond.^{67,68} Although the B–N bond is isoelectronic with the C–C bond, it is significantly weaker as a result of poor orbital overlap. Nevertheless, there is evidence that such dative bonds can alter the pharmacological activity of boronic acids and esters.^{69,70} Since no data were available on the structure of $\text{H}_2\text{N}-\text{CH}_2-\text{CH}=\text{CH}-\text{B}(\text{OH})_2$, we initially optimized the geometry of a variety of its conformers. The lowest-energy form, R(1), of this boronic acid in vacuo was consistently found to be a seven-membered, hydrogen-bonded ring structure in which the boronic acid moiety is in a trigonal planar arrangement; see Figure 1; the calculated $\text{H}\cdots\text{N}$ distance and $\text{O}\cdots\text{H}-\text{O}$ angle are indicative of a relatively strong hydrogen bond.^{71,72} Such a seven-membered ring motif has been

observed in the crystal structure of an R,R-bisboronic acid by Zhao et al.⁷³ and predicted in gas-phase computational studies of 2-aminocarbonylphenylboronic acid by Bhat et al.⁶⁷

The computational levels we employed in this investigation, however, differed on which conformer of $\text{H}_2\text{N}-\text{CH}_2-\text{CH}=\text{CH}-\text{B}(\text{OH})_2$ was closest in energy to R(1) in the gas phase: (PBE1PBE)[MP2] favored a dative-bonded five-membered ($:\text{N}-\text{C}-\text{C}=\text{C}-\text{B}$) cyclic structure, R(2), whereas B3LYP favored an acyclic structure, R(3) (see Figure 1); relative energies of R(1)–R(3) are listed in Table 1. Differences among these levels are not surprising, because there is evidence suggesting that the B3LYP functional underestimates the strength of dative bonds involving boron;⁶⁷ indeed, the optimized B–N distance in R(2) is ~ 0.01 Å longer at the B3LYP level than it is at the MP2 level. Interestingly, we also found another local minimum, R(2'), on the B3LYP PES with the same basic structure as R(2) (see Figure 1), but where the B–N distance, 2.65 Å, was very long (experimental B–N dative bond lengths range from ~ 1.76 to 1.84 Å^{74–77}); R(2') was 0.8 kcal/mol *lower* in energy than R(2). R(2'), however, was not found to be a local minimum at the (PBE1PBE)[MP2] levels. Thus, B3LYP does not find a substantial stabilizing effect from a $\text{B}\cdots\text{N}$ interaction at a distance of 1.83 Å. The Höpft index,⁷⁸ $\text{THC}_{\text{DA}}[\%]$, for the tetrahedral character of the boron atom in R(2), 49.4% (52.8%)-[53.2%], indicates that it has substantial tetrahedral character. However, the nitrogen and oxygen atoms in this boronic acid all carry significant negative charge and these atoms are in relatively close proximity in R(2); the electrostatic repulsion in this compact cyclic conformer certainly contributes to the fact that it is *not* the global minimum on the PES of $\text{H}_2\text{N}-\text{CH}_2-\text{CH}=\text{CH}-\text{B}(\text{OH})_2$ in vacuo.⁵⁰

Since the lengths of B–N dative bonds are known to depend on their environment,⁷⁹ conformers R(1)–R(3) of $\text{H}_2\text{N}-\text{CH}_2-\text{CH}=\text{CH}-\text{B}(\text{OH})_2$ were reoptimized in the reaction field of water. The optimized B–N bond length of R(2) was consistently computed to be shorter in aqueous media than was it was in vacuo (see Table 1); similar behavior has been observed with the intermolecular adduct $\text{H}_3\text{B}\cdot\text{NH}_3$.^{79,80} Interestingly, in aqueous media the dative-bonded conformer R(2) was predicted to be [2.2] kcal/mol *lower* in energy than the hydrogen-bonded conformer R(1) at the [MP2] computational level; at the (PBE1PBE) level these conformers have nearly the same energy, whereas at the B3LYP level R(2) is 3.6 kcal/mol *higher* in energy than R(1); conformer R(3) is higher in energy than either R(1) or R(2) at all three levels. Although the predicted energy differences among conformers R(1)–R(3) depend on the computational methodology employed, they all suggest that the dative-bonded conformer R(2) plays a greater role in the chemistry of $\text{H}_2\text{N}-\text{CH}_2-\text{CH}=\text{CH}-\text{B}(\text{OH})_2$ in aqueous media than it does in vacuo; explicitly hydrated zwitterionic forms of this acid will be discussed later.⁸¹

(61) Cances, E.; Mennucci, B.; Tomasi, J. *J. Chem. Phys.* **1997**, *107*, 3032.

(62) Cossi, M.; Barone, V.; Mennucci, B.; Tomasi, J. *Chem. Phys. Lett.* **1998**, *286*, 253.

(63) Cossi, M.; Scalmani, G.; Rega, N.; Barone, V. *J. Chem. Phys.* **2002**, *117*, 43.

(64) Mennucci, B.; Tomasi, J. *J. Chem. Phys.* **1997**, *106*, 5151.

(65) Castejon, H.; Wiberg, K. B. *J. Am. Chem. Soc.* **1999**, *121*, 2139.

(66) Castejon, H.; Wiberg, K. B.; Sklenak, S.; Hinz, W. *J. Am. Chem. Soc.* **2001**, *123*, 6092.

(67) Bhat, K. L.; Howard, N. J.; Rostami, H.; Lai, J. H.; Bock, C. W. *J. Mol. Struct. (THEOCHEM)* **2005**, *723*, 147.

(68) Franzen, S.; Ni, W.; Wang, B. *J. Phys. Chem. B* **2003**, *107*, 12942.

(69) Kelly, T. A.; Adams, J.; Bachovchin, W. W.; Barton, R. W.; Campbell, S. J.; Coutts, S. J.; Kennedy, C. A.; Snow, R. J. *J. Am. Chem. Soc.* **1993**, *115*, 12637.

(70) Snow, R. J.; Bachovchin, W. W.; Barton, R. W.; Campbell, S. J.; Freeman, D. M.; Gutheil, W. G.; Kelly, T. A.; Kennedy, C. A.; Krolkowski, D. A.; Leonard, S. F.; Pargellis, C. A.; Tong, L.; Adams, J. *J. Am. Chem. Soc.* **1994**, *116*, 10860.

(71) Kyte, J. *Structure in Protein Chemistry*; Garland Publishers: New York, 1995.

(72) Rettig, S. J.; Trotter, J. *Can. J. Chem.* **1977**, *55*, 3071.

(73) Zhao, J.; Davidson, M. G.; Mahon, M. F.; Kociok-Kohn, G.; James, T. D. *J. Am. Chem. Soc.* **2004**, *126*, 16179.

(74) For comparison we note that the B–N bond length in $\text{H}_2\text{B}\cdot\text{NH}_2$ is 1.39 Å at the B3LYP computational level.

(75) Norrild, J. C.; Sjötofte, I. *J. Chem. Soc., Perkin Trans.* **2002**, *2*, 303.

(76) Toyota, S.; Asakura, M.; Futawaka, T.; Oki, M. *Bull. Chem. Soc. Jpn.* **1999**, *72*, 1879.

(77) Toyota, S.; Oki, M. *Bull. Chem. Soc. Jpn.* **1992**, *65*, 1832.

(78) Höpfl, H. *J. Organomet. Chem.* **1999**, *581*, 121.

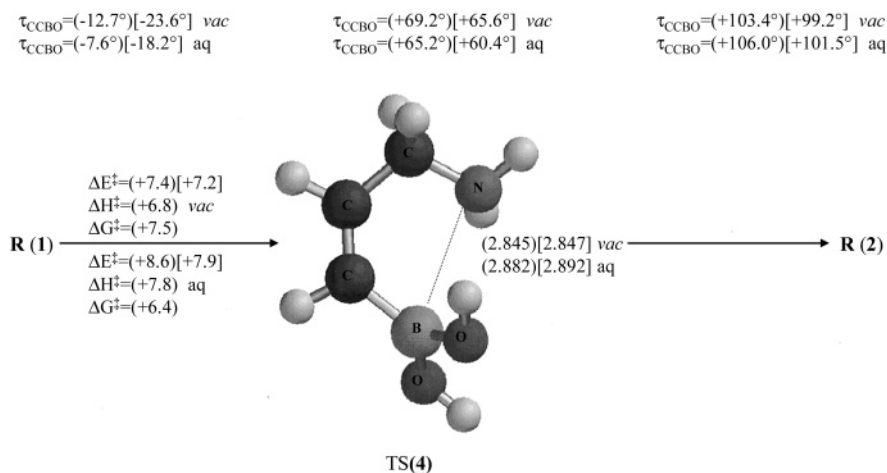
(79) Bühl, M.; Steinke, T.; Schleyer, P. V.; Boese, R. *Angew. Chem., Int. Ed. Engl.* **1991**, *30*, 1160.

(80) Ahlrichs, R.; Furche, F.; Grimme, S. *Chem. Phys. Lett.* **2000**, *325*, 317.

Table 1. Relative Energies, E_{rel} (kcal/mol), B–N Distances (Å), and τ_{CCCN} and τ_{CCCB} Torsional Angles (deg) for Selected Conformers of $\text{H}_2\text{N}-\text{CH}_2-\text{CH}_2-\text{CH}=\text{CH}-\text{B}(\text{OH})_2$

conformer	vacuo				aqueous media (SCRF:PCM)			
	E_{rel}	B–N	τ_{CCCN}	τ_{CCCB}	E_{rel}	B–N	τ_{CCCN}	τ_{CCCB}
R(1) B3LYP	0.0	3.248	42.2	2.0	0.0	3.197	29.7	2.4
(PBE1PBE)	0.0	3.207	39.3	2.8	+0.0 ₂	3.162	28.3	3.0
[MP2]	0.0	3.249	57.8	2.4	+2.2	3.179	47.0	2.4
R(2) B3LYP	+7.1	1.829 ^a	−6.6	−1.4	+3.6	1.736	−6.9	−1.5
(PBE1PBE)	+3.6	1.752	−8.2	−1.5	0.0	1.707	−6.6	−1.8
[MP2]	+2.3	1.728	−12.0	−1.9	0.0	1.695	−10.6	−2.3
R(3) B3LYP	+3.5	4.907	−121.0	179.2	+3.0	4.919	−122.3	179.5
(PBE1PBE)	+4.2	4.882	−121.6	179.1	+4.0	4.896	−123.2	179.6
[MP2]	+4.8	4.878	−118.7	178.9	+5.9	4.887	−119.8	179.2

^a A second local minimum R(2') with a structure similar to that of R(2) was found in the gas phase at the B3LYP level. The five-membered (:N–C=C–B) ring in R(2') is "open"; that is, the B–N distance is 2.65 Å. This conformer is 0.8 kcal/mol lower in energy than R(2).

**Figure 2.** Transition state (TS(4)) for the conformer conversion R(1)→R(2) of $\text{H}_2\text{N}-\text{CH}_2-\text{CH}=\text{CH}-\text{B}(\text{OH})_2$. (Atomic distances are given in angstroms (Å), torsional angles are in degrees (°), and energies are in kcal/mol at the (PBE1PBE)[MP2] computational levels.)**Table 2. Reaction Energies (kcal/mol) for the Intramolecular Cyclization Reaction**

reaction		vacuo			aqueous SCRF		
		ΔE	ΔH°_{298}	ΔG°_{298}	ΔE	ΔH°_{298}	ΔG°_{298}
R(2) → P(5) + H ₂ O	B3LYP	+6.8	+4.6	−5.6	+7.4	+4.7	−5.7
	(PBE1PBE)	+10.0	+7.6	−2.8	+11.0	+8.3	−2.4
	[MP2]	+11.7 ^a			+12.6 ^a		
reaction		ΔE^\ddagger	ΔH^\ddagger	ΔG^\ddagger	ΔE^\ddagger	ΔH^\ddagger	ΔG^\ddagger
R(2) → TS(6)	B3LYP	+30.8	+27.1	+28.2	+34.4	+30.2	+30.4
	(PBE1PBE)	+28.9	+25.2	+26.0	+33.1	+28.9	+29.5
	[MP2]	+30.3			+34.6		

^a ΔE is [+3.7] in vacuo and [9.2]kcal/mol in the reaction field of water at the [MP2] level for the reaction R(2) → P(5)⋯H₂O, where P(5)⋯H₂O is a hydrogen-bonded adduct between P(5) and H₂O.

The transition state TS(4) for the interconversion of the hydrogen-bonded and dative-bonded conformers, R(1) and R(2), respectively, is shown in Figure 2. It involves a rotation about the C–B bond and is (7.4)[7.2] kcal/mol higher in energy than R(1) in vacuo and (8.6)[7.9] kcal/mol higher in energy in the reaction field of water at the (PBE1PBE)[MP2] levels.⁸²

The structure and relative energies of various conformers of the product ether, $\text{H}_2\text{N}-\text{CH}_2-\text{CH}=\text{CH}-\text{B}(\text{OH})(\text{OCH}_3)$, mimic those of the reactant acid: the corresponding seven-membered, hydrogen-bonded ring structure is lowest in energy in vacuo, whereas a B–N dative-bonded structure is lowest in energy in aqueous media at the [MP2] level; see Table 2S.⁸³ Interestingly,

(81) Typically, SCRF methods are not as reliable in protic solvents such as H₂O because the model assumes that the solvent molecules adopt all possible random orientations with respect to the solute.^{65,66}

(82) At the B3LYP level in vacuo, the conversion appears to occur in two steps; the barrier for the initial step is 7.5 kcal/mol.

B–N distances are generally found to be slightly longer in the ether than in the acid both in vacuo and in aqueous media; Franzen et al.⁶⁸ have reported similar results for the *o*-(trimethylamino)phenylboronic acid/ester model system.

B. Intramolecular Dehydration Reaction. Boronic acids containing the $\text{H}_2\text{N}-\text{CH}_2-\text{C}\equiv\text{C}-\text{B}(\text{OH})_2$ structural unit, where the C≡C bond is part of an aromatic system, can undergo unimolecular dehydration in aprotic solvents to yield five-membered heterocyclic structures.^{84,85} These experimental results prompted us to establish the energetics of such an intramolecular process for $\text{H}_2\text{N}-\text{CH}_2-\text{CH}=\text{CH}-\text{B}(\text{OH})_2$. We envisioned

(83) In vacuo, however, no B–N dative-bonded structure was found at the B3LYP level, stressing again that care must be exercised in using this functional for both aminoboronic acids and ethers and, by implication, for esters.

(84) Hawkins, R. T.; Blackham, A. U. *J. Org. Chem.* **1967**, *32*, 597.

(85) Hawkins, R. T.; Synder, H. R. *J. Am. Chem. Soc.* **1960**, *82*, 3863.

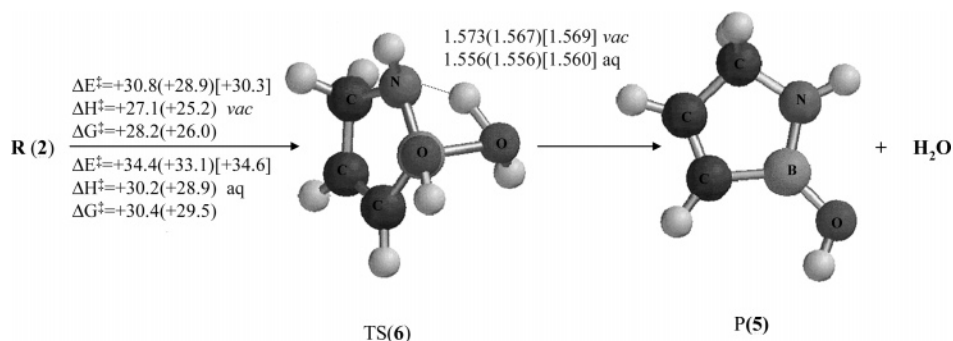


Figure 3. Unimolecular water elimination reaction for conformer R(2) of H₂N–CH₂–CH=CH–B(OH)₂. (Atomic distances are given in angstroms (Å), and energies are in kcal/mol at the B3LYP(PBE1PBE)[MP2] computational levels.)

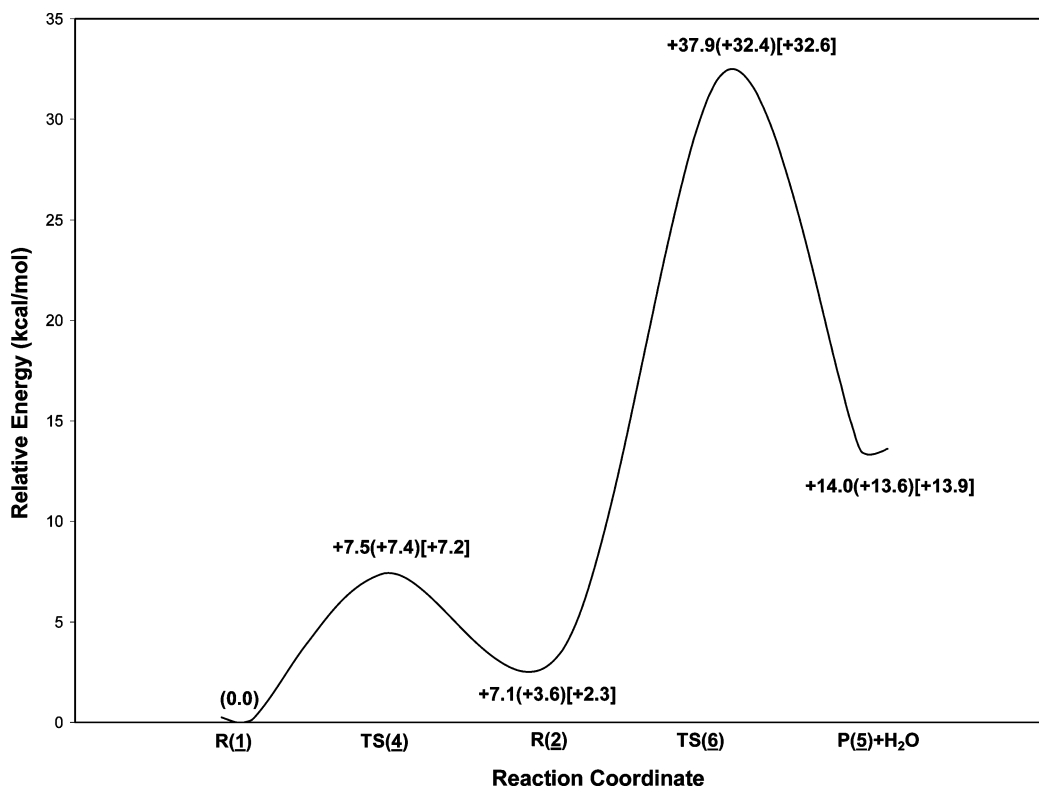


Figure 4. Relative energy (kcal/mol) diagram for the R(1)→R(2) conversion and the unimolecular dehydration of the dative-bonded conformer R(2) of H₂N–CH₂–CH=CH–B(OH)₂ in vacuo to give (–HN–CH₂–CH=CH–)B(OH), P(5), at the B3LYP(PBE1PBE)[MP2] computational levels.

the formation of a product ring structure (–HN–CH₂–CH=CH–)B(OH), P(5), from the compact reactant conformer R(2).

The structure of the ring in P(5) was nearly planar; the computed length of the B–N bond was quite short, ~1.4 Å, both in the gas phase and in the reaction field of water; NBO analyses indicated that it was a double bond. In vacuo, the values of ΔH^\ddagger_{298} and ΔG^\ddagger_{298} for the elimination reaction were +4.6(+7.6) and –5.6(–2.8) kcal/mol, respectively, at the B3LYP(PBE1PBE) levels. The transition state, TS(6), for this process is shown in Figure 3, and the value of ΔG^\ddagger in vacuo, +28.2(+26.0) kcal/mol, was quite high; see Figure 4. In aqueous media the energetics of this unimolecular dehydration reaction were similar to those in vacuo; see Table 2.

C. Methanolysis of H₂N–CH₂–CH=CH–B(OH)₂. The methanolysis of H₂N–CH₂–CH=CH–B(OH)₂, in vacuo and in aqueous media, will be discussed separately.

C.1. In Vacuo. Several mechanisms for the methanolysis, H₂N–CH₂–CH=CH–B(OH)₂ + H₃C–OH → H₂N–CH₂–CH=CH–B(OH)–(OCH₃) + H₂O, were investigated. These mechanisms differ in the role played by the primary amine group

during the process; no experimental thermochemical data are available for comparison.

C.1.1. Catalyzed Mechanism. We considered first a pathway for the methanolysis of H₂N–CH₂–CH=CH–B(OH)₂, in which the primary amine group played a catalytic role. This mechanism was initiated from the lowest-energy, hydrogen-bonded conformer R(1); it involved a series of steps associated with breaking the intramolecular N···H hydrogen bond in R(1) and orienting the methanol to form an intermolecular B–O dative-bonded adduct, AD(7); see Figure 5A. The activation barriers from separated R(1) and H₃C–OH to AD(7) were relatively low in energy (see Figure 6), and the kinetics of the methanolysis is controlled by a subsequent 1,3-proton transfer. The optimized B–O(H)(CH₃) distance in AD(7) was relatively short, and NBO analyses indicated the presence of a B–O dative bond; the boron atom had considerable tetrahedral character, the value of the Höpft index being (59.3%)[63.7%] at the (PBE1PBE)[MP2] levels.⁷⁸ Even though the methanol moiety also donates a

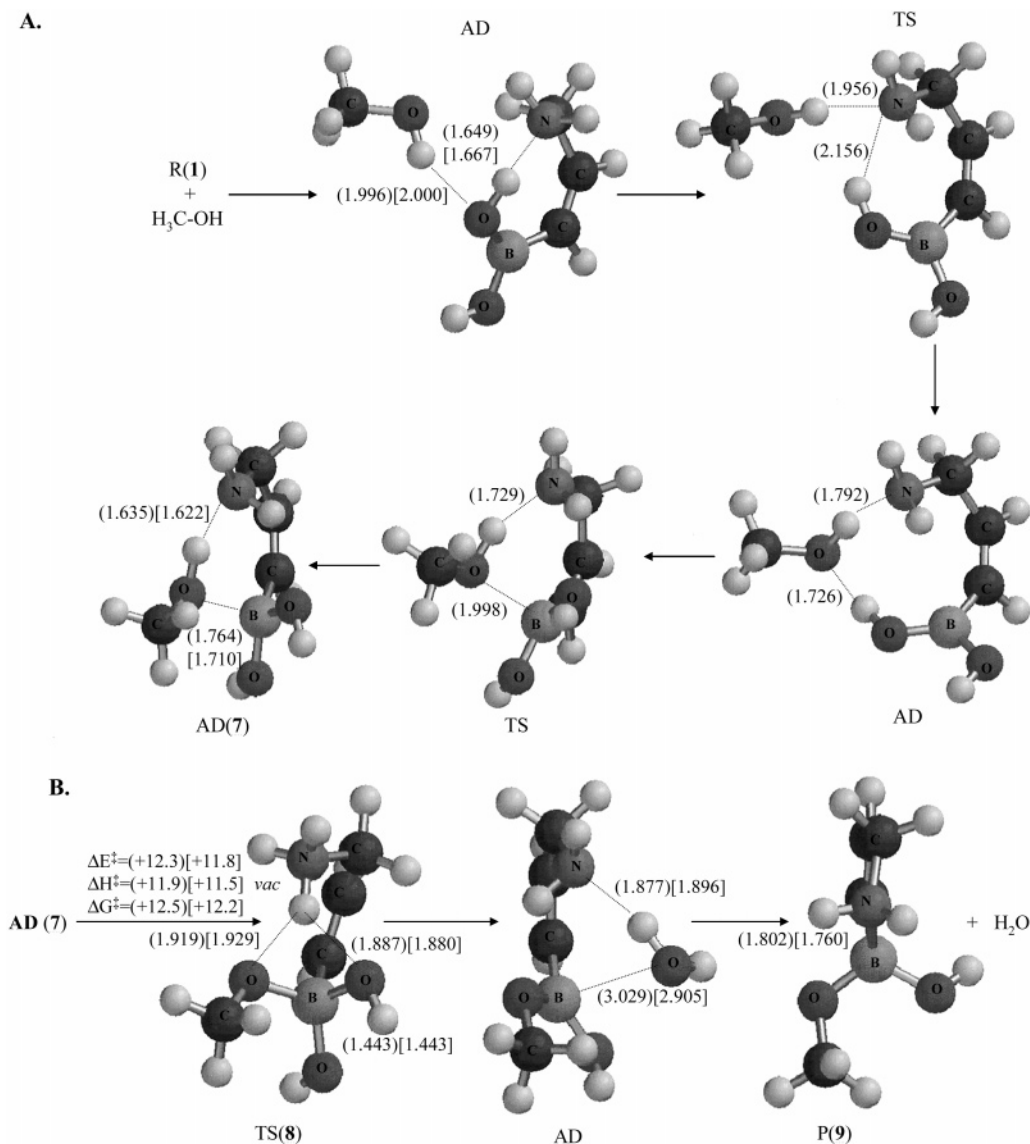


Figure 5. Catalyzed methanolysis mechanism for (A) the conversion of isolated R(1) and H₃C–OH to the dative-bonded adduct AD(7) and (B) the 1,3-proton shift initiated from AD(7) leading to the product P(9). (Atomic distances are given in angstroms (Å) and energies are in kcal/mol at the B3LYP(PBE1PBE)[MP2] computational levels.)

hydrogen bond to the amine nitrogen atom in AD(7), it is only (0.2)[3.9] kcal/mol lower in energy than the separated reactants.⁸⁶

The structure of the transition state, TS(8), for the rate-determining, proton-transfer step in the methanolysis is shown in Figure 5B. The role of the amine group in this transition state is clearly to facilitate the proton transfer; indeed, the proton being transferred was only ~ 1.05 Å from the nitrogen atom, and its distance from each of the oxygen atoms involved in the transfer was ~ 1.9 Å. Thus, the structure of TS(8) suggests that an $-\text{NH}_3^+$ moiety is effectively present, and the net NPA charge on this group, $(+0.62e)[+0.62e]$, supports this interpretation. Despite the zwitterionic-like structure of TS(8) in vacuo, it was only (12.0)[7.9] kcal/mol higher in energy than the isolated reactants at the (PBE1PBE)[MP2] levels, and the free energy of activation from AD(7), $(+12.5)[+12.2]$ kcal/mol, was relatively low; see Table 3.⁸⁷ It is important to note that there was a significant increase in the tetrahedral character of the

boron atom in TS(8) compared to that in AD(7); the value of the Hüpft index jumped to (77.4%)[78.7%].⁸⁸

This proton transfer leads to a hydrogen-bonded adduct between the product ether, H₂N–CH₂–CH=CH–B(OH)–(OCH₃), and H₂O that is (12.6)[11.1] kcal/mol lower in energy

(87) For a more basic tertiary amine, with $-\text{NH}_2$ replaced by $-\text{N}(\text{CH}_3)_2$, the analogous transition state is only (7.5) kcal/mol higher in energy than the corresponding reactants at the (PBE1PBE) computational level.

(88) Details of this catalyzed mechanism are somewhat different when the B3LYP functional is employed. Starting from the (PBE1PBE) geometry of AD(7), the B3LYP optimization resulted in a hydrogen-bonded adduct in which the boronic acid moiety is trigonal planar; this adduct is (3.4) kcal/mol lower in energy than separated R(1) and H₃C–OH, and no B–O dative bond is present in the NBO analysis of this structure. Thus, the hybrid B3LYP functional appears to underestimate the strength of a dative bond involving boron when compared to the corresponding ab initio MP2 result. A stable dative-bonded form was located on the B3LYP PES when the conformation of the boronic acid moiety was changed to eliminate the intramolecular hydrogen bond between the two hydroxyl groups bound to the boron atom, but it is 8.2 kcal/mol higher in energy than R(1) and methanol. The proton transfer from this adduct proceeds in two steps: the methanolic hydrogen is first transferred to the nitrogen atom ($E^\ddagger = 2.5$ kcal/mol), leading to a stable zwitterion, and then one of the protons originally covalently bound to the nitrogen is transferred to one of the hydroxyl groups on the boron atom ($E^\ddagger = 4.9$ kcal/mol).

(86) When the $-\text{CH}_3$ group in AD(7) is replaced by $-\text{H}$, and the structure is reoptimized, the resulting R(1)···H₂O adduct is held together by hydrogen bonds only.

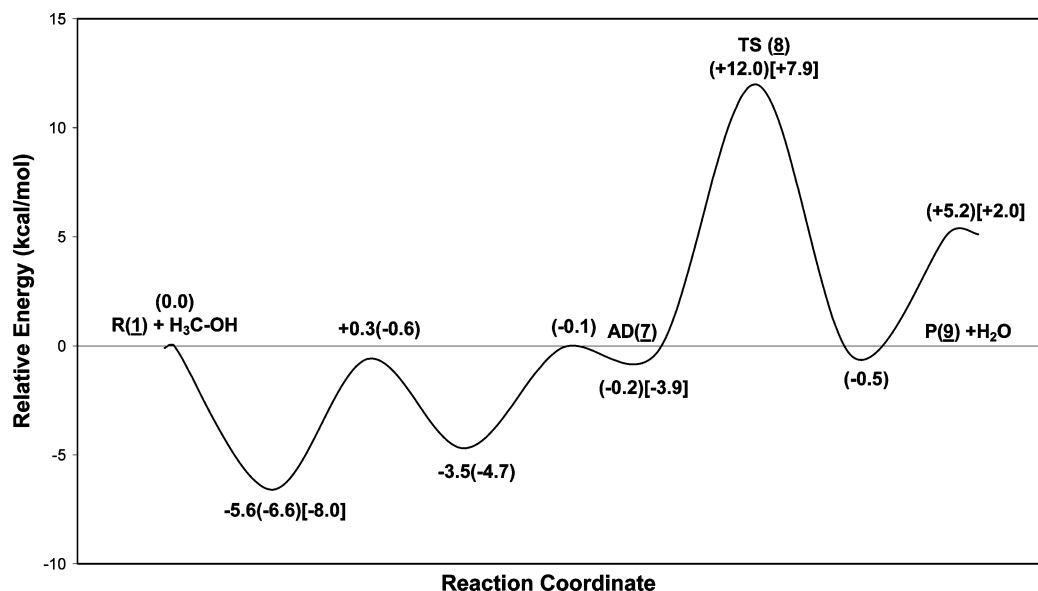


Figure 6. Relative energy (kcal/mol) diagram for the catalyzed methanolysis of conformer R(1) of $\text{H}_2\text{N}-\text{CH}_2-\text{CH}=\text{CH}-\text{B}(\text{OH})_2$ at the B3LYP(PBE1PBE)[MP2] computational levels.

Table 3. Reaction Energetics (kcal/mol) for the Intermolecular Dehydration Reaction

reaction		vacuo		
		ΔE	ΔH^\ddagger_{298}	ΔG^\ddagger_{298}
R(1) + $\text{H}_3\text{C}-\text{OH} \rightarrow \text{P}(9) + \text{H}_2\text{O}$	B3LYP	+6.8	+5.6	+5.7
	(PBE1PBE)	+5.2	+4.0	+5.3
	[MP2]	+2.0		
reaction		ΔE^\ddagger	ΔH^\ddagger	ΔG^\ddagger
AD(7) \rightarrow TS(8) (catalyzed)	B3LYP	+12.3	+11.9	+12.5
	(PBE1PBE)	+11.8	+11.5	+12.2
	[MP2]			
AD(11) \rightarrow TS(10) (uncatalyzed)	B3LYP	+29.2	+25.6	+30.1
	(PBE1PBE)	+27.8		
	[MP2]			
AD(13) \rightarrow TS(12) (uncatalyzed)	B3LYP	+35.3	+31.4	+33.7
	(PBE1PBE)	+30.9	+27.2	+29.0
	[MP2]			

than TS(8); no B–O dative-bonded adduct between the products could be located. On the other hand, removing the H_2O moiety from this adduct and geometry optimizing the remaining structure gave the B–N dative-bonded product P(9) at the (PBE1PBE)[MP2] computational levels; see Figure 5B and Table 2S. The B–N distance in this product is (1.80)[1.76] Å, and a B–N dative-bonding orbital is evident in the NBO analysis of P(9).

C.1.1. Uncatalyzed Mechanisms. Two gas-phase mechanisms for the methanolysis of $\text{H}_2\text{N}-\text{CH}_2-\text{CH}=\text{CH}-\text{B}(\text{OH})_2$ were investigated in which the amine group did not play a direct catalytic role. The first of these was biased to keep the seven-membered hydrogen-bonded ring structure in R(1) intact during the process. The transition state, TS(10), for the rate-determining proton-transfer step is shown in Figure 7A; the corresponding adduct, AD(11), which was (6.1)[7.1] kcal/mol lower in energy than the isolated reactants, was hydrogen-bonded rather than dative-bonded. TS(10) involved a compact four-membered ring; for example, the proton being transferred was only ~ 1.2 Å from the two oxygen atoms involved compared to ~ 1.9 Å in TS(8), and the value of the Höpft index for the boron atom in TS(10), (53.1%)[53.7%] at the (PBE1PBE)[MP2] levels, was more than 20% lower than it is in TS(8). TS(10) was (23.1)[20.7] kcal/mol higher in energy than separated R(1) and methanol, and it was (11.0)[12.8] kcal/mol higher in energy on the PES than TS(8). The ether product, $\text{H}_2\text{N}-\text{CH}_2-\text{CH}=\text{CH}-\text{B}(\text{OH})(\text{OCH}_3)$,

involved an intramolecular, seven-membered, hydrogen-bonded ring structure similar to that found in R(1), and it was (0.8) kcal/mol lower in energy than the dative-bonded form of the product, P(9).

The second uncatalyzed mechanism had the amine group positioned so that it could not interact directly with either the boronic acid moiety or the methanolic hydrogen atom. The transition state, TS(12), is shown in Figure 7B; the corresponding adduct, AD(13), between $\text{H}_2\text{N}-\text{CH}_2-\text{CH}=\text{CH}-\text{B}(\text{OH})_2$ and $\text{H}_3\text{C}-\text{OH}$, was doubly hydrogen-bonded rather than dative-bonded. The structure of AD(13) and the $\text{H}_2\text{N}-\text{CH}_2-\text{CH}=\text{CH}-\text{B}(\text{OH})_2$ reactant involved an intramolecular $\text{O}\cdots\text{HC}$ hydrogen bond in a six-membered ring motif; this conformer of the acid is (6.0) kcal/mol higher in energy than R(1). TS(12) is (21.7) kcal/mol higher in energy than the separated reactants, and it is (15.7)[17.3] kcal/mol higher in energy than TS(8). The ether product generated via this mechanism also involves a six-membered ring with an $\text{O}\cdots\text{HC}$ hydrogen bond; it is (2.9) kcal/mol higher in energy than P(9).

The number of rotatable bonds in $\text{H}_2\text{N}-\text{CH}_2-\text{CH}=\text{CH}-\text{B}(\text{OH})_2$ and the potential for intramolecular/intermolecular hydrogen- and dative-bond formation suggest that other mechanisms for the methanolysis are possible; those described above, however, are likely to be representative. Our results indicate that transition states for the rate-determining proton-transfer step for the methanolysis of $\text{H}_2\text{N}-\text{CH}_2-\text{CH}=\text{CH}-\text{B}(\text{OH})_2$ in vacuo

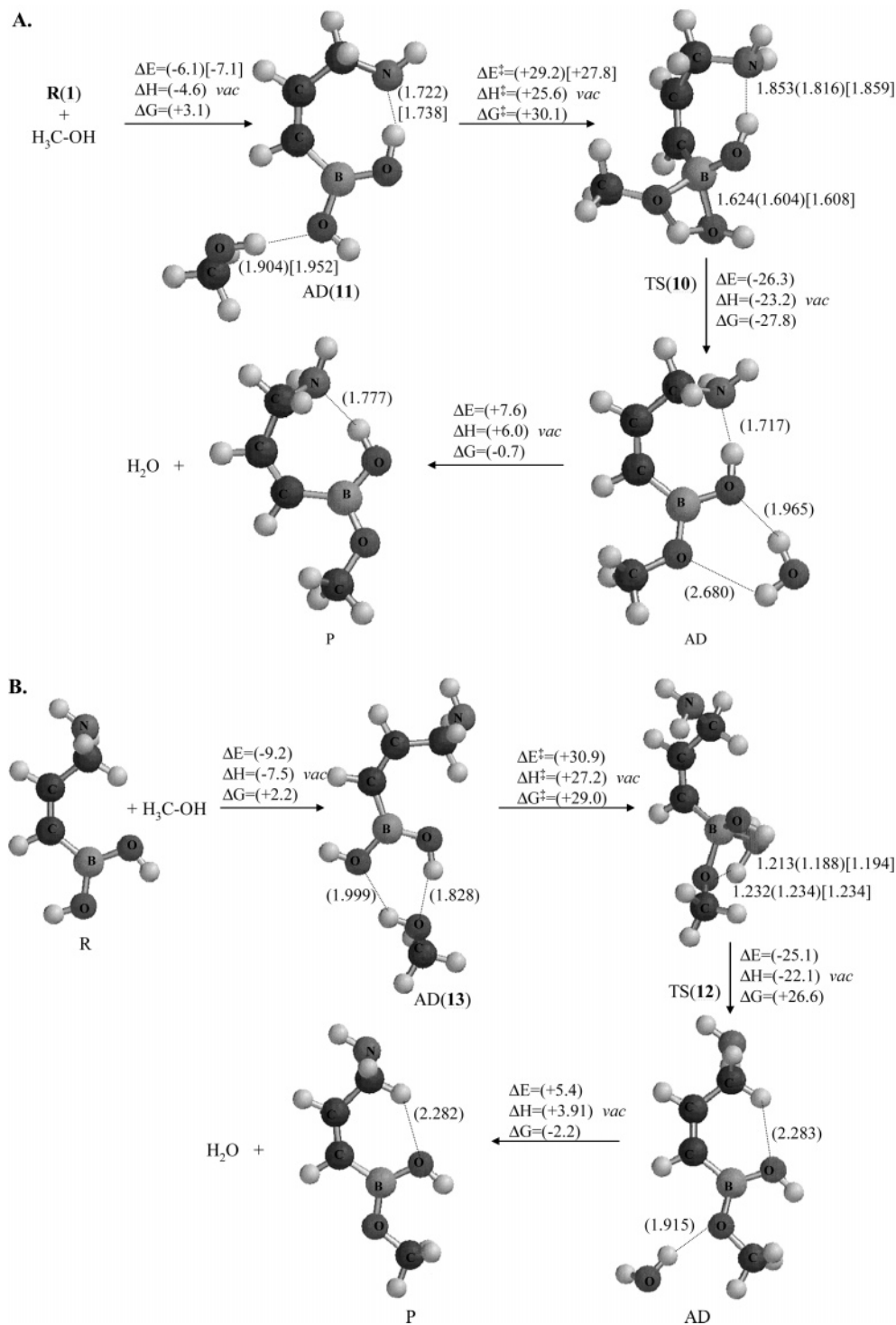


Figure 7. Uncatalyzed methanolysis mechanism for (A) the conversion of isolated R(1) and H₃C–OH to the corresponding hydrogen-bonded conformer of the product and H₂O and (B) the conversion of a six-membered hydrogen-bonded conformer of the reactant, H₂N–CH₂–CH=CH–B(OH)₂ and H₃C–OH, to the corresponding conformer of the product and H₂O. (Atomic distances are given in angstroms (Å) and energies are in kcal/mol at the B3LYP(PBE1PBE)[MP2] computational levels.)

are significantly higher in energy, $\sim(11-16)[13-17]$ kcal/mol, in the absence of an internal primary amine to act as a Lewis base. To further validate this conclusion, we located the transition state for a 1,3-proton shift involved in the methanolysis of the related compound H₃C–CH=CH–B(OH)₂, in which *no* amine group is available to act in a catalytic role; the transition state is (21.5) kcal/mol higher in energy than the separated reactants at the (PBE1PBE) level, which is in accord with our results for the uncatalyzed methanolysis mechanisms of H₂N–CH₂–CH=CH–B(OH)₂.

C.2. In Aqueous Media. Many factors involved in the association of boronic acids with diols in aqueous media, particularly when a nitrogenous base is proximal to the boron center, are not well understood; for example, Franzen et al.⁶⁸ recently suggested that B–N dative bonds may *not* be present in the structures of boronate esters formed between *o*-aminomethylphenyl boronic acids and saccharide molecules due to competing solvolysis processes. Even less is known about the analogous association of boronic acids with aliphatic alcohols in aqueous solution. As noted above for the free acid, the seven-

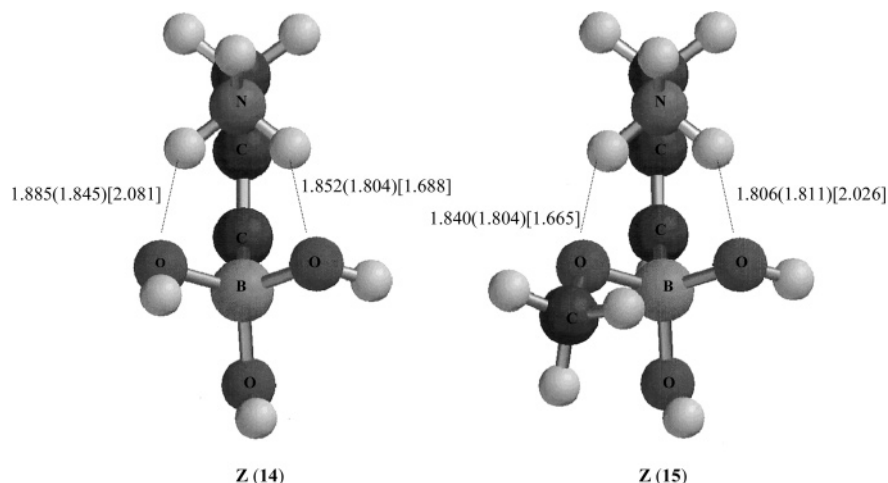


Figure 8. Structures of the zwitterions $\text{H}_3\text{N}^+-\text{CH}_2-\text{CH}=\text{CH}-\text{B}(\text{OH})_3^-$ and $\text{H}_3\text{N}^+-\text{CH}_2-\text{CH}=\text{CH}-\text{B}(\text{OH})_2(\text{OCH}_3)^-$. (Atomic distances are given in angstroms (Å) at the B3LYP(PBE1PBE)[MP2] computational levels.)

membered hydrogen-bonded and the five-membered dative-bonded ring conformers, R(1) and R(2), respectively, are predicted to be closer in energy in the reaction field of water than they are in vacuo, and the dative-bonded form is predicted to be lower in energy than the hydrogen-bonded form at the [MP2] level; see Table 1. These calculations, however, were carried out using a continuum model, and the results are more representative of a high-dielectric aprotic solvent than of water, which can form specific, directional bonds.

To gain further insight into the importance of solvolysis, SCRF geometry optimizations were performed for conformers of $\text{H}_2\text{N}-\text{CH}_2-\text{CH}=\text{CH}-\text{B}(\text{OH})_2$ and $\text{H}_2\text{N}-\text{CH}_2-\text{CH}=\text{CH}-\text{B}(\text{OH})(\text{OCH}_3)$ in the presence of an explicit water molecule. The boron atoms in the resulting zwitterions, $\text{H}_3\text{N}^+-\text{CH}_2-\text{CH}=\text{CH}-\text{B}(\text{OH})_3^-$, Z(14), and $\text{H}_3\text{N}^+-\text{CH}_2-\text{CH}=\text{CH}-\text{B}(\text{OH})_2(\text{OCH}_3)^-$, Z(15), are nearly tetracoordinated (see Figure 8); the values of the H \ddot{o} pf index were 83.2% (82.8%)[82.7%] and 83.0% (83.1%)[81.7%], respectively. Using the lowest-energy B–N dative-bonded conformers of $\text{H}_2\text{N}-\text{CH}_2-\text{CH}=\text{CH}-\text{B}(\text{OH})_2$ and $\text{H}_2\text{N}-\text{CH}_2-\text{CH}=\text{CH}-\text{B}(\text{OH})(\text{OCH}_3)$, SCRF calculations indicated that the simple hydration reactions, $\text{H}_2\text{N}-\text{CH}_2-\text{CH}=\text{CH}-\text{B}(\text{OH})_2 + \text{H}_2\text{O} \rightarrow \text{H}_3\text{N}^+-\text{CH}_2-\text{CH}=\text{CH}-\text{B}(\text{OH})_3^-$ and $\text{H}_2\text{N}-\text{CH}_2-\text{CH}=\text{CH}-\text{B}(\text{OH})(\text{OCH}_3) + \text{H}_2\text{O} \rightarrow \text{H}_3\text{N}^+-\text{CH}_2-\text{CH}=\text{CH}-\text{B}(\text{OH})_2(\text{OCH}_3)^-$, are nearly thermoneutral; the values of ΔE are +0.3(–0.5)[–0.1] and +0.3(–0.6)[+0.3] kcal/mol, respectively, at the B3LYP(PBE1PBE)-[MP2] levels. Furthermore, the exchange reaction, $\text{H}_3\text{N}^+-\text{CH}_2-\text{CH}=\text{CH}-\text{B}(\text{OH})_3^- + \text{H}_3\text{C}-\text{OH} \rightarrow \text{H}_3\text{N}^+-\text{CH}_2-\text{CH}=\text{CH}-\text{B}(\text{OH})_2(\text{OCH}_3)^- + \text{H}_2\text{O}$, is also nearly thermoneutral in the reaction field of water; the values of ΔE , ΔH°_{298} , and ΔG°_{298} are (–0.2), (–0.5), and (+1.3) kcal/mol, respectively, showing that the methyl group has only a modest influence on the stability of the zwitterion. Transition states for the conversion of the zwitterion $\text{H}_3\text{N}^+-\text{CH}_2-\text{CH}=\text{CH}-\text{B}(\text{OH})_2(\text{OCH}_3)^-$ into the acid $\text{H}_2\text{N}-\text{CH}_2-\text{CH}=\text{CH}-\text{B}(\text{OH})_2$ and $\text{H}_3\text{C}-\text{OH}$, or into the ether $\text{H}_2\text{N}-\text{CH}_2-\text{CH}=\text{CH}-\text{B}(\text{OH})(\text{OCH}_3)$ and H_2O , are only (2.3) kcal/mol and (4.2) kcal/mol, respectively, higher in energy than $\text{H}_3\text{N}^+-\text{CH}_2-\text{CH}=\text{CH}-\text{B}(\text{OH})_2(\text{OCH}_3)^-$. These results indicate that zwitterionic species of aminoboric acids and ethers, in which there is no B–N dative bond in the structure, may play a more important role in the aqueous chemistry of these acids than previously thought. This finding is in accord with those of Franzen et al.,⁶⁸ who found that the mechanism of action for the electron-transfer quenching of anthracene fluorescence involves explicit interactions with

solvent water molecules rather than with the formation of intramolecular B–N dative bonds.

We also investigated a mechanism for the methanolysis of $\text{H}_2\text{N}-\text{CH}_2-\text{CH}=\text{CH}-\text{B}(\text{OH})_2$ in the reaction field of water that was biased to keep the seven-membered, hydrogen-bonded ring structure of R(1) intact; the transition state for this pathway, analogous to that of TS(10), was (29.8) kcal/mol higher in energy than R(1) and methanol at the SCRF (PBE1PBE) level.

Concluding Remarks

Experimentally, it is well established that the formation of boronate esters from boronic acids and vicinal diols is sensitive to pH²¹ and that internal Lewis bases can be effective in lowering the pH required to form stable boronic acid–diol complexes.^{42,43} Results of the calculations reported in this article for the methanolysis of the aminoboric acid $\text{H}_2\text{N}-\text{CH}_2-\text{CH}=\text{CH}-\text{B}(\text{OH})_2$ to form the ether $\text{H}_2\text{N}-\text{CH}_2-\text{CH}=\text{CH}-\text{B}(\text{OH})(\text{OCH}_3)$, in which the primary aliphatic amine acts as an internal Lewis base to catalyze the process, provide computational support and mechanistic insight into these experimental findings.

The structure of $\text{H}_2\text{N}-\text{CH}_2-\text{CH}=\text{CH}-\text{B}(\text{OH})_2$ has not been established experimentally. In vacuo the lowest-energy conformer, R(1), was a seven-membered, hydrogen-bonded ring structure^{67,73} at the computational levels we employed; a five-membered B–N dative-bonded conformer, R(2), was found to be [2.3] kcal/mol *higher* in energy at the [MP2] computational level, suggesting that the B–N dative bond in this case was somewhat weaker than a hydrogen bond. By contrast, SCRF calculations in aqueous media find R(2) to be [2.3] kcal/mol *lower* in energy than R(1).

In vacuo, the catalytic role of the primary amine group in the methanolysis of $\text{H}_2\text{N}-\text{CH}_2-\text{CH}=\text{CH}-\text{B}(\text{OH})_2$ results from facilitation of a proton transfer from an intermolecular B–O dative-bonded adduct between methanol and this boronic acid (see Figure 5) rather than from the formation of an intramolecular B–N dative-bonded structure. In two distinct mechanisms for the methanolysis, in which the amine group was positioned to reduce its effectiveness as a catalyst, the transition states for the proton-transfer step were [12.8] and [17.3] kcal/mol higher in energy than the corresponding transition state for the catalyzed reaction. In aqueous media, the competition between seven-membered hydrogen-bonded, five-membered B–N dative-bonded, and hydrated zwitterionic species appears to be rather complex. Additional experimental and computational

results will be necessary to identify the influence of these various species on chemosensor and therapeutic function. Molecular dynamics simulations of an aminoboronic acid in an aqueous environment would be useful, but the available molecular mechanics parameters for boron are quite limited and need to be enhanced in view of recent developments.^{89–92}

Finally, we note that the B3LYP functional produces anomalous results in some instances compared to those from the more robust, albeit expensive, MP2 method, particularly when a B–N dative interaction is present. However, this does not appear to be an inherent limitation of currently available DFT methods, since the PBE1PBE functional gives results in excellent

agreement with those obtained from ab initio MP2 calculations and, thus, appears to be an economical alternative for modeling more extended boronic acid systems.

Acknowledgment. K.L.B. would like to thank the National Textile Center (C03-PH01) and G.D.M. would like to thank the NIH (GM31186, CA06927) and NCI for financial support of this work, which was also supported by an appropriation from the Commonwealth of Pennsylvania.

Supporting Information Available: A listing of molecular energies of all species studied (Table 1S), relative energies and geometrical parameters of conformers of H₂N–CH₂–CH=CH–B(OH)(OCH₃) (Table 2S), and geometries of the species studied in PDF format are available free of charge via the Internet at <http://pubs.acs.org>.

OM0509239

(89) Chen, X.; Liang, G.; Whitmire, D.; Bowen, J. P. *J. Phys. Org. Chem.* **1998**, *11*, 378.

(90) Fisher, L.; Holme, T. *J. Comput. Chem.* **2001**, *22*, 913.

(91) James, J. J.; Whiting, A. *J. Chem. Soc., Perkin Trans.* **1996**, *2*, 1861.

(92) Otkidach, D. S.; Pletnew, I. V. *J. Mol. Struct. (THEOCHEM)* **2001**, *536*, 65.